Key role of barstar Cys-40 residue in the mechanism of heat denaturation of bacterial ribonuclease complexes with barstar

I.I. Protasevich[a], A.A. Schulga[b], L.I. Vasilieva[b], K.M. Polyakov[c], V.M. Lobachov[a], R.W. Hartley[d], M.P. Kirpichnikov[b], A.A. Makarov[a],*

[a]*Engelhardt Institute of Molecular Biology, Russian Academy of Sciences, 117984 Moscow, Russia*
[b]*Shemyakin-Ovchinnikov Institute of Bioorganic Chemistry, Russian Academy of Sciences, 117871 Moscow, Russia*
[c]*Institute of Crystallography, Russian Academy of Sciences, 117333 Moscow, Russia*
[d]*National Institute of Diabetes and Digestive and Kidney Diseases, National Institutes of Health, Bethesda, MD 20892, USA*

Abstract The mechanism by which barnase and binase are stabilized in their complexes with barstar and the role of the Cys-40 residue of barstar in that stabilization have been investigated by scanning microcalorimetry. Melting of ribonuclease complexes with barstar and its Cys-82-Ala mutant is described by two 2-state transitions. The lower-temperature one corresponds to barstar denaturation and the higher-temperature transition to ribonuclease melting. The barstar mutation Cys-40-Ala, which is within the principal barnase-binding region of barstar, simplifies the melting to a single 2-state transition. The presence of residue Cys-40 in barstar results in additional stabilization of ribonuclease in the complex.
© 1999 Federation of European Biochemical Societies.

Key words: Barnase; Binase; Barstar mutant;
Protein-protein complex; Thermal denaturation

1. Introduction

Many crucial biological processes are based on protein-protein interactions. As a model system of protein-protein recognition, the complex of *Bacillus amyloliquefaciens* ribonuclease (barnase) with its protein inhibitor barstar is currently widely used [1,2]. In this paper the molecular mechanism of the stabilizing effect of protein-protein interactions was studied on heat denaturation of complexes formed by barnase and related *Bacillus intermedius* ribonuclease (binase) with barstar and its Cys→Ala mutants. Scanning differential microcalorimetry, which allows monitoring of the system melting and estimation of the contribution of individual components, was used.

The primary structures of barnase and binase differ in 17 residues, but substitutions are outside the active site of the enzymes. Three-dimensional structures of these ribonucleases both in the free state and in complexes with substrate analogs have been established [3–5]. Despite high homology of amino acid sequences and similarity of spatial structures, essential differences in their enzymatic properties and stability were found [6]. Barstar is a natural inhibitor of barnase protecting *B. amyloliquefaciens* cells against lethal effects of the enzyme's expression. It forms a one-to-one non-covalent complex with barnase with a dissociation constant of about 10^{-14} M [1,2]. Barstar is also able to inhibit binase, and constants of barstar binding to barnase and binase are close to each other [7].

Barstar contains two cysteine residues at positions 40 and 82 forming no disulfide bond [8,9]. NMR did not reveal any marked differences between barstar and its double mutant, in which cysteine residues were replaced by alanines (Cys-40,82-Ala) [10,11]. The spatial structure of the barnase complex with Cys-40,82-Ala barstar was determined by X-ray analysis [12,13]. This complex is formed by sterically blocking the enzyme active site by a relatively small continuous polypeptide fragment of the inhibitor (amino acid residues 29–46). As shown in [13], an additional interaction between catalytically active His-102 of barnase and Cys-40 of barstar may appear upon formation of barnase complex with barstar.

2. Materials and methods

2.1. Protein expression and purification

The construction of expression plasmids for barnase and binase as well as the procedure for their purification have been described [6]. Expression plasmids for barstar and its Cys→Ala variants were constructed by replacement of gene 10 in pGEMEX1 (Promega) by the barstar gene from pMT316 [14]. Barstar and its mutants were purified from *Escherichia coli* strain BL21(DE3) harboring the corresponding expression plasmid. Harvested cells were disrupted by ultrasonication. Nucleic acids were precipitated by gradual addition of polyethyleneimine to a final concentration of 0.04%. Cleared lysate was fractionated with ammonium sulfate. The protein fraction precipitated in the saturation interval 40–80% was purified on a Superose 12 prep grade column (Pharmacia) followed by dialysis and gradient chromatography on MonoQ HR10/10 (Pharmacia). Peak fractions were pooled, exhaustively dialyzed against 10 mM EDTA, pH 7.5, and lyophilized. The resulting protein was essentially pure in SDS-PAGE. The barstar purification was carried out in the presence of 50 mM dithiothreitol (DTT) at all steps, except final dialysis. Mass spectrometry has shown that barstar and its mutants still have the N-terminal methionine. Protein solutions were prepared in 10 mM Na-acetate, 0.05 M NaCl, pH 6.2. In some cases denaturation was studied in the presence of 1 mM DTT. Protein concentration was determined with a Jasco V-550 spectrophotometer, assuming the following molar extinction at 280 nm (in M^{-1} cm^{-1}): 27411 for barnase and binase [6], 22959 for barstar, 22714 for Cys-40,82-Ala barstar, 23301 for Cys-40-Ala barstar, and 22270 for Cys-82-Ala barstar [15].

2.2. Scanning microcalorimetry

Microcalorimetric measurements were carried out on a DASM-4 differential scanning microcalorimeter (NPO Biopribor, Pushchino, Russia) in 0.48 ml cells at a heating rate of 1 K/min or in some cases 0.5 and 2.0 K/min. Ribonuclease concentration was 0.4–0.5 mg/ml, whereas that of barstar and its mutants was 0.6–0.8 mg/ml. The reversibility of the unfolding was checked routinely by sample reheating after cooling in the calorimetric cell. The partial molar heat capacity of the protein (C_p), denaturation temperature (T_d), calorimetric denaturation enthalpy (ΔH_{cal}), and effective or van't Hoff denaturation enthalpy (ΔH_{eff}) were determined as described elsewhere [16]. The accuracy of the calorimetric and effective enthalpies was ±6%, that of T_d within ±0.2°C. To analyze functions of excess heat capacity, we

*Corresponding author. Fax: (7) (095) 135-1405.
E-mail: aamakarov@genome.eimb.relarn.ru

used the SCAL2 software package developed at the Institute of Protein Research (Pushchino, Russia). The errors in the parameters of individual transitions obtained by deconvolution of ribonuclease-barstar complex melting curves did not exceed ±10% for transition enthalpy and ±0.6°C for transition temperature.

2.3. Circular dichroism (CD)

CD spectra were recorded on a Jasco J-715 spectropolarimeter equipped with the thermostatted water-jacketed cells (Hellma Cells, USA) and Neslab RTE-111 programmable circulating water bath (Neslab Instruments, USA). The cells had the light path of 0.02 and 1.0 cm, protein concentration was 0.6–0.8 mg/ml. For continuous melting of the samples, the temperature was increased at 1 K/min and the transition temperatures were determined from the peaks on the first temperature derivatives of the normalized melting profiles. The results were expressed as molar ellipticity, $[\Theta]$ (deg cm^2 dmol^{-1}), based on mean amino acid residue weights of 114.7 for barstar and 114.0 for Cys-40,82-Ala barstar.

3. Results and discussion

3.1. Heat denaturation of free barstar and its Cys→Ala mutants

The barstar and Cys-40,82-Ala barstar CD spectra in the wavelength interval 185–250 nm coincide with each other (Fig. 1, curves 1, 4), as could be expected, since no disulfide bond was formed by the replaced cysteine residues [8]. CD spectra of barstar mutants with the single substitutions Cys-40-Ala and Cys-82-Ala appeared to be similar to those of barstar [9]. The barstar CD spectra with two minima at 208 and 220 nm and a big maximum near 193 nm are characteristic of α-helical proteins. Fig. 1 (inset) shows the barstar and Cys-40,82-Ala barstar melting curves by the CD change at 220 nm. Denaturation temperatures of barstar (73.0±0.4°C) and Cys-40,82-Ala barstar (73.7±0.4°C) are practically identical. Fig. 1 (curves 2, 5) shows that there are no marked differences between the barstar and Cys-40,82-Ala barstar CD spectra registered at 90°C. However, melting of the Cys-40,82-Ala barstar secondary structure was almost 90% reversible (curve 3), whereas that for barstar reached only 60% (curve 6).

Earlier, we failed in calorimetric determination of parameters of the wild-type barstar heat denaturation at pH 6.2 due to aggregation of denatured protein molecules [17]. Addition of the reducing agent DTT allowed us to register the barstar
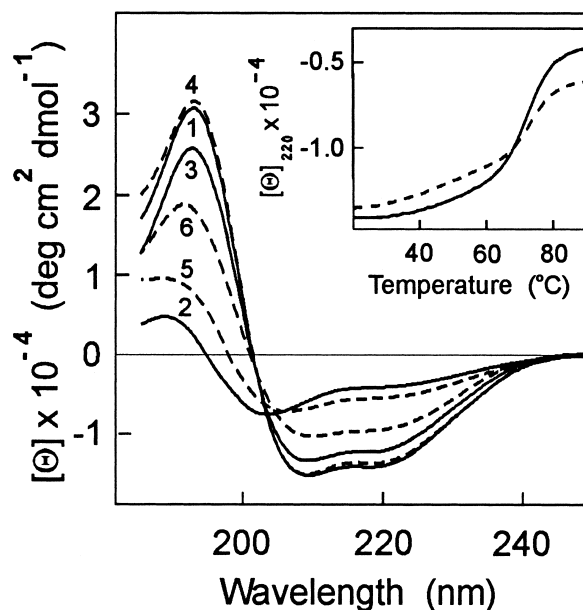

Fig. 1. CD spectra of barstar (dotted lines) and Cys-40,82-Ala barstar (solid lines) in the far-UV region at pH 6.2 and 20°C (1, 4), 90°C (2, 5), and after cooling from 90°C to 20°C (3, 6). The inset shows the temperature dependence of CD at 220 nm for barstar (dotted line) and Cys-40,82-Ala barstar (solid line). $[\Theta]_{220}$ is given in the same units as $[\Theta]$.

melting curve (Fig. 2, curve 1). The reversibility of Cys-40,82-Ala barstar denaturation was almost complete (97%), whereas for barstar it reached only 60%, which correlates with the CD data. The barstar denaturation temperature coincides with that obtained from CD (Table 1) and is equal to the temperature of the first deconvoluted peak of calorimetric curve of barnase-barstar complex (Table 2). This confirms our previous conclusion that the first deconvoluted peak of the ribonuclease-barstar complex melting curve corresponds to denaturation of barstar [7,17]. Melting temperatures of barstar and Cys-40,82-Ala barstar are the same and, taking into account the stabilizing effect of NaCl, they are close to those described in [18,19]. As the melting temperatures of the single barstar mutant Cys-40-Ala and the wild-type protein are close to each

Table 1
Thermal denaturation parameters of free binase, barnase, barstar and its Cys→Ala mutants and their complexes at pH 6.2

Sample	T_d (°C)	ΔH_{cal} (kcal/mol)	ΔH_{eff} (kcal/mol)	R^a
Barstar[b]	73.3 (73.0[c])	53	76	0.70
Cys-40,82-Ala barstar	73.6 (73.7[c])	73	71	1.03
Cys-82-Ala barstar[b]	71.9	49	68	0.72
Cys-40-Ala barstar[b]	74.1	51	73	0.70
Binase	56.5	124	126	0.98
Barnase	54.5	129	130	0.99
Binase+Cys-40,82-Ala barstar	76.6	191	182	1.05
Binase+Cys-40-Ala barstar	76.5	185	169	1.09
Barnase+Cys-40,82-Ala barstar	74.5	203	167	1.22
Barnase+Cys-40-Ala barstar	75.3	186	161	1.16
Binase+barstar	83.3	195	77	2.53
Binase+Cys-82-Ala barstar	81.5	191	98	1.95
Barnase+barstar	78.4	250	111	2.25
Barnase+barstar[b]	78.3	250	124	2.02
Barnase+Cys-82-Ala barstar	76.7	211	105	2.01

[a] $R = \Delta H_{cal}/\Delta H_{eff}$.
[b] In the presence of 1 mM DTT.
[c] Values of denaturation temperature obtained from the CD change at 220 nm.
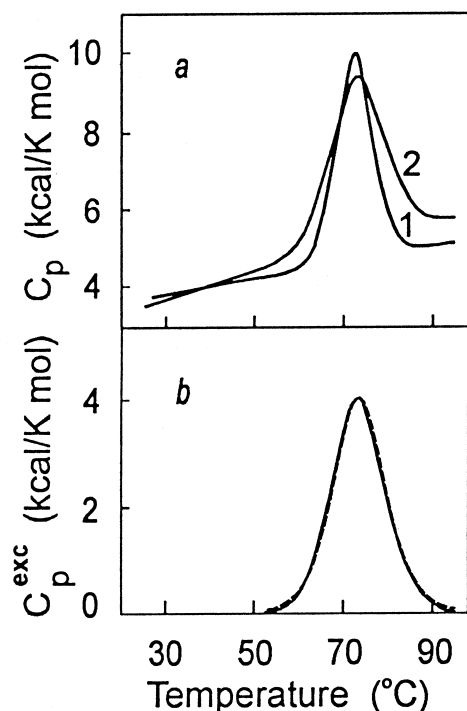
Fig. 2. Temperature dependence of the partial molar heat capacity of barstar (curve 1) and Cys-40,82-Ala barstar (curve 2) at pH 6.2 (a). Computer deconvolution of the transition excess heat capacity of Cys-40,82-Ala barstar (b): experimental curve (solid line) and the curve calculated assuming that unfolding is a 2-state transition (dotted line).

other, that of Cys-82-Ala barstar is 1.4°C lower than barstar denaturation temperature (Table 1). The latter was also demonstrated in [20].

The $\Delta H_{cal}/\Delta H_{eff}$ (R) ratio, which relates to the number of cooperative units in the molecule [16], is equal to 1 for Cys-40,82-Ala barstar, and the melting curve is well described by the transition between two states (Fig. 2b), whereas R for barstar is essentially below 1 (Table 1). The denaturation enthalpy for barstar is almost 30% lower than that for Cys-40,82-Ala barstar, whereas their effective enthalpy values are identical. This is indicative of the association of denatured barstar molecules, probably due to intercysteine S-S bond formation. Thus, substitution of both cysteines in the barstar molecule with alanines results in increased reversibility of protein melting without changes in its thermal stability.

3.2. Heat denaturation of free barnase and binase

We have shown earlier [6] that although there is a high degree of homology between primary and three-dimensional structures, the thermal stability of binase at pH 5.5 exceeds that of barnase by 2°C. The same difference of melting temperatures was registered at pH 6.2 (Table 1). The R value for ribonuclease denaturation is equal to 1 (Table 1) in spite of a relatively incomplete melting reversibility in the presence of 0.05 M NaCl (64% and 73% for binase and barnase, respectively). The change in the heating rate in the range of 0.5–2.0 K/min had no effect on heat denaturation parameters of ribonucleases. Hence, the process leading to a slight decrease in the denaturation reversibility is slower than the denaturation proper, and thus it does not influence its parameters.

3.3. Heat denaturation of barnase and binase complexes with barstar and its Cys → Ala mutants

Fig. 3 shows the temperature dependences of the partial molar heat capacity of barnase (a) and binase (b) complexes with Cys-40,82-Ala (1) and wild-type barstar (2) at pH 6.2. The reversibility of melting of barnase complexes with barstar and its double mutant reached 50–55% due to incomplete reversibility under these conditions of one or both free proteins. Addition of DTT, which markedly decreases self-association of denatured barstar molecules, did not influence the parameters and reversibility of barnase-barstar complex melting (Table 1). This result supports our previous conclusion that interaction with barnase prevents barstar from self-association during denaturation [17]. Melting of binase complexes with barstar and Cys-40,82-Ala barstar was completely irreversible, but neither melting temperature, nor enthalpy depended on the heating rate (0.5–2.0 K/min), which makes possible the thermodynamic analysis of the calorimetric curves.

Melting curves of ribonuclease complexes with Cys-40,82-Ala barstar (Fig. 3a,b, curves 1) are shifted to lower temperatures by 3.9°C for barnase complexes and by 6.7°C for those of binase, as compared with the thermograms of complexes with barstar (curves 2), and essentially differ in shape. The R ratio for ribonuclease complexes with barstar is higher than 2 (Table 1), which suggests the existence of more than one cooperative transition. Computer deconvolution of the excess
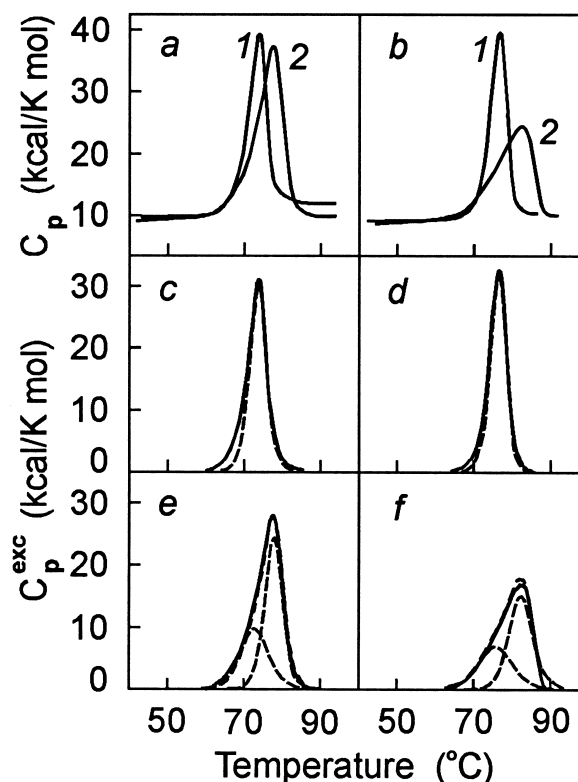

Fig. 3. Temperature dependence of the partial molar heat capacity of barnase (a) and binase (b) complexes with Cys-40,82-Ala barstar (1) and barstar (2) at pH 6.2. Computer deconvolution of the transition excess heat capacity of barnase complexes with Cys-40,82-Ala barstar (c) and barstar (e) and binase complexes with Cys-40,82-Ala barstar (d) and barstar (f): experimental curves (solid lines), deconvoluted peaks corresponding to the 2-state transitions, and their sum (dotted lines).

heat capacity function for these complexes into individual 'all-or-none' transitions shows that melting curves of the complexes may be presented as two 2-state transitions (Fig. 3e,f). According to our previous data [7,17], the lower-temperature deconvoluted peak is indicative of barstar denaturation, whereas the higher-temperature one corresponds to ribonuclease melting. After denaturation, barstar is still bound to ribonuclease. At the second step this weakened complex dissociates and denaturation of ribonuclease takes place [7,17]. This model is based on the fact that barnase is bound to barstar residues located at a relatively short region of the polypeptide chain (residues 29–46) [12]. Presumably this region of barstar is also stabilized and remains intact independently of the rest of the molecule.

Unlike ribonuclease complexes with the wild-type barstar, the effective enthalpy indicating the size of a cooperatively melted unit is markedly higher, and R value is close to 1 for complexes with Cys-40,82-Ala barstar (Table 1). As for the binase-Cys-40,82-Ala barstar complex, we obtained excellent coincidence of its experimental melting curve with that calculated assuming that unfolding is a 2-state transition (Fig. 3d). Thus, heat denaturation of the binase-Cys-40,82-Ala barstar complex is realized according to the 'all-or-none' principle, i.e. the complex is melted as a single cooperative system. Although there is a slight asymmetry of the barnase-Cys-40,82-Ala barstar melting curve and R=1.2, its deconvolution does not allow one to distinguish two transitions, and the curve is quite well approximated by a single 2-state transition (Fig. 3c). The difference between the experimental and calculated curves may be indicative of formation during denaturation of the complex of some molecules in the intermediate thermodynamically stable condition. Thus, the melting mechanisms of ribonuclease complexes with barstar and Cys-40,82-Ala barstar differ in principle, and in the complex with the double mutant both the inhibitor and enzyme are melted at the same temperature.

Our data on denaturation of ribonuclease complexes with single Cys→Ala barstar mutants indicate that the complex with the Cys-40-Ala mutant is melted similarly to that with Cys-40,82-Ala barstar, whereas the complex with the Cys-82-Ala mutant resembles that with wild-type barstar (Table 1). Thus, the barstar residue Cys-40 is responsible for realization in two 2-state transitions of the heat denaturation of ribonuclease-barstar complex. The 1.7–1.8°C decrease of denaturation temperature of ribonuclease complexes with Cys-82-Ala barstar is evidently predetermined by the 1.4°C lowering of the uncomplexed mutant denaturation temperature as compared with the wild-type protein.

Thermodynamic parameters of transitions obtained from deconvolution of the excess heat capacity function of binase and barnase complexes with barstar and Cys-82-Ala barstar are given in Table 2. Melting temperatures of free barstar and its Cys-82-Ala mutant coincide with those for complexes with
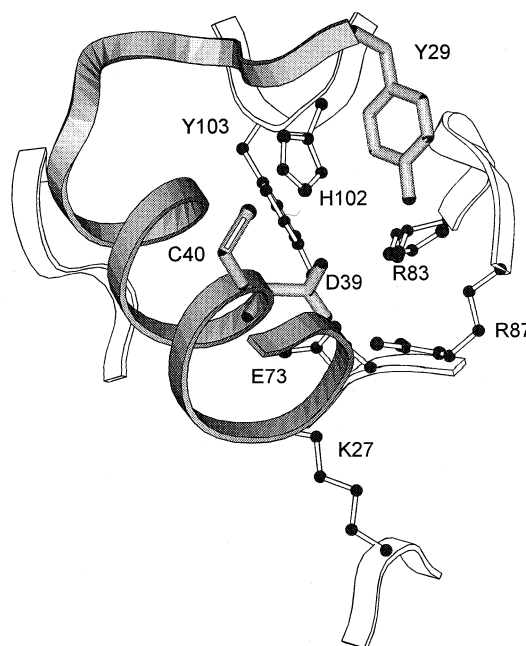

Fig. 4. The environment of barnase His-102 residue in its complex with barstar. The coordinates of the barnase-Cys-40,82-Ala barstar complex were used [12]. Coordinates of barstar Cys-40 were obtained by computer modeling. The side chain of Cys-40 is turned to provide for the shortest distance to His-102. The barnase and barstar main chains are shown as ribbon models, white and gray, respectively. Side chains of barstar residues in the contact region (Tyr-29, Asp-39, and Cys4-0) are shown as a bulk model, whereas those of barnase (Lys-27, Glu-73, Arg-83, Arg-87, His-102, and Tyr-103) are represented as balls and sticks.

barnase (Tables 1 and 2), which correlates with the X-ray data about insignificant structural alterations in barstar upon its binding to barnase [21]. Unlike this, formation of barstar and its Cys→Ala mutant complexes with binase results in an increase of thermal stability of inhibitor by 2.4–4.2°C. The enthalpies of binase and barnase binding to barstar are also different [7]. Barstar is not a natural inhibitor of binase, and the differences in the properties of its complexes with barnase and binase could be expected. All barnase residues taking part in its interaction with barstar are also present in binase, except Ser-85 and Gln-104 which are involved only in van der Waals contacts in the barnase-barstar complex and are replaced by alanines in binase [12]. Unfortunately, the structure of the binase-barstar complex is unknown, and this does not allow us to correlate the observed differences in the properties of binase and barnase complexes with their structure. The difference in thermal stability between free binase and barnase equal to 2°C (Table 1) is increased to 4.6°C for their complexes with barstar, but it is not changed in those with Cys-40,82-Ala barstar.

Table 2
Thermodynamic parameters of transitions obtained by deconvolution of excess heat capacity function for binase and barnase complexes with barstar and its Cys-82-Ala mutant

Complex	T_d^1 (°C)	ΔH_d^1 (kcal/mol)	T_d^2 (°C)	ΔH_d^2 (kcal/mol)
Binase+barstar	75.8	82	82.4	124
Binase+Cys-82-Ala barstar	76.1	83	81.2	127
Barnase+barstar	72.8	87	77.8	154
Barnase+Cys-82-Ala barstar	73.0	76	75.0	160

3.4. The role of barstar residue Cys40 in ribonuclease stabilization upon complex formation

The melting temperatures of barnase and binase are increased for 23.3°C and 25.9°C, respectively, in their complexes with barstar and for 20°C in those with Cys-40,82-Ala barstar (Tables 1 and 2). Since barstar and Cys-40,82-Ala barstar are characterized by equal thermal stabilities, one may suppose that the higher stabilizing effect of barstar is caused by the greater number of contacts with ribonuclease. In fact, the comparison of the crystal structure of the barnase-Cys-40,82-Ala barstar complex with that of free wild-type barstar and free barnase has shown [13] that the sulfur atom in the barstar Cys-40 may form a hydrogen bond with the side chain of the catalytic His-102 in barnase. Computer modeling of the barnase-barstar complex, based on the structure of the barnase-Cys-40,82-Ala barstar complex, shows that the His-102 side chain in barnase and the sulfur atom in barstar Cys-40 are in close contact, and electrostatic interaction between them becomes possible (Fig. 4). The absence of this bond in the case of Cys-40,82-Ala barstar weakens its interaction with ribonucleases, which also corresponds to the lower constant of this mutant association with barnase [1,13]. During denaturation, the Cys-40 stabilizing effect can favor preservation of the native conformation of the inhibitor binding site which causes the difference in the heat denaturation mechanisms of complexes with barstar and Cys-40,82-Ala barstar. The results of melting of ribonuclease complexes with single Cys → Ala barstar mutants (Table 1) fully support the key role of residue Cys-40 in ribonuclease stabilization within the complex and realization of one or another mechanism of complex melting.

The facts that denaturation of ribonuclease within its complex with the wild-type barstar takes place after melting of the inhibitor, and the region of ribonuclease contact with barstar includes the active site of the enzyme, suggest that the latter may be the region of initial unfolding of the globule upon heat denaturation. This is in coincidence with the lower thermal stability of ribonuclease in the complex with Cys-40,82-Ala and Cys-40-Ala barstars in the absence of the enzyme catalytic histidine interaction with Cys-40 of the inhibitor.

References

[1] Hartley, R.W. (1993) Biochemistry 32, 5978–5984.
[2] Schreiber, G. and Fersht, A.R. (1993) Biochemistry 32, 5145–5150.
[3] Guillet, V., Lapthorn, A. and Mauguen, Y. (1993) FEBS Lett. 330, 137–140.
[4] Buckle, A.M. and Fersht, A.R. (1994) Biochemistry 33, 1644–1653.
[5] Pavlovsky, A.G., Borisova, S.N., Strokopytov, B.V., Sanishvili, R.G., Vagin, A.A. and Chepurnova, N.K. (1988) in: Metabolism and Enzymology of Nucleic Acids (Zelinka, J. and Balan, J., Eds.), pp. 217–222, Plenum Press, New York.
[6] Schulga, A., Kurbanov, F., Kirpichnikov, M., Protasevich, I., Lobachov, V., Ranjbar, B., Chekhov, V., Polyakov, K., Engelborghs, Y. and Makarov, A. (1998) Protein Eng. 11, 775–782.
[7] Yakovlev, G.I., Moiseyev, G.P., Protasevich, I.I., Ranjbar, B., Kirpichnikov, M.P., Gilli, R.M., Briand, C.M., Hartley, R.W. and Makarov, A.A. (1995) FEBS Lett. 366, 156–159.
[8] Frisch, C., Schreiber, G. and Fersht, A.R. (1995) FEBS Lett. 370, 273–277.
[9] Ramachandran, S. and Udgaonkar, J.B. (1996) Biochemistry 35, 8776–8785.
[10] Lubienski, M., Bycroft, M., Freund, S.M.V. and Fersht, A.R. (1994) Biochemistry 33, 8866–8877.
[11] Wong, K.-B., Fersht, A.R. and Freund, S.M.V. (1997) J. Mol. Biol. 268, 494–511.
[12] Guillet, V., Lapthorn, A., Hartley, R.W. and Mauguen, Y. (1993) Structure 1, 165–177.
[13] Buckle, A.M., Schreiber, G. and Fersht, A.R. (1994) Biochemistry 33, 8878–8889.
[14] Hartley, R.W. (1988) J. Mol. Biol. 202, 913–915.
[15] Martinez, J.C., Filimonov, V.V., Mateo, P.L., Schreiber, G. and Fersht, A.R. (1995) Biochemistry 34, 5224–5233.
[16] Privalov, P.L. and Potekhin, S.A. (1986) Methods Enzymol. 131, 4–51.
[17] Makarov, A.A., Protasevich, I.I., Lobachov, V.M., Kirpichnikov, M.P., Yakovlev, G.I., Gilli, R.M., Briand, C.M. and Hartley, R.W. (1994) FEBS Lett. 354, 251–254.
[18] Khurana, R., Hate, A.T., Nath, U. and Udgaonkar, J.B. (1995) Protein Sci. 4, 1133–1144.
[19] Wintrode, P.L., Griko, Yu.V. and Privalov, P.L. (1995) Protein Sci. 4, 1528–1534.
[20] Schoppe, A., Hinz, H.J., Agashe, V.R., Ramachandran, S. and Udgaonkar, J.B. (1997) Protein Sci. 6, 2196–2202.
[21] Ratnaparkhi, G.S., Ramachandran, S., Udgaonkar, J.B. and Varadarajan, R. (1998) Biochemistry 37, 6958–6966.